GLACIOLOGIC AND PALEOCLIMATIC SIGNIFICANCE OF CIRQUE-LAKE SEDIMENTS IN THE ALBION RANGE, SOUTH-CENTRAL IDAHO

PAUL BOVET
Colorado College, Colorado Springs
Sponsor: Eric Leonard, Colorado College

NICOLE BOWERMAN
Western Washington University, Bellingham
Sponsor: Doug Clark, Western Washington University

DANIEL CADOL
Whitman College
Sponsor: Robert Carson, Whitman College

INTRODUCTION

The Albion Range in south-central Idaho supported two separate centers of alpine glaciation during the late Pleistocene, at Cache Peak (10,399'; 3170 m) and at Mt. Harrison (9265', 2824 m). Both peaks have well developed cirques on their northeastern slopes that contain moraine-dammed lakes: the four Independence Lakes in the cirque between Cache Peak and Independence Peak, and Lake Cleveland in a deep valley below Mt. Harrison (Fig. 1). These cirques hosted small valley glaciers during the late-Wisconsin glacial maximum (Pinedale equivalent), which left behind complex sets of recessional moraines as they retreated at the close of the Pleistocene.

In an effort to establish numerical constraints on glaciation and climate change since the late Pleistocene in this region, our group investigated the extent and timing of the Pinedale maximum and related recessional moraines. Moraine mapping, combined with known characteristics of modern alpine glaciers, allows us to estimate past glacial snowlines and climate conditions related to these events. To constrain the timing of the demise of these glaciers, and to investigate environmental conditions since the glaciers disappeared, we also collected sediment cores from each of the five lakes. Bathymetric surveys of the lakes allowed us to target the deepest parts of basins within the lakes. The glaciolacustrine approach of our study provides constraints on conditions both at the last glacial maximum, as well as a continuous record of environmental change since that time. Our sedimentologic analyses of long cores from the three largest lakes includes visual stratigraphy, magnetic susceptibility, sediment grain size, and organic carbon content.

Organization

Because our study required the integration of several complex and logistically difficult elements, our group worked throughout the project as a team ("Team Mud"). As a result, our abstract consists of both jointly written group sections (Introduction, Methodology, Conclusions), as well as individual sections (sections 1-3, identified by author). We emphasize, however, that even the individual sections include work by all members of the team, and therefore we use plural tense in much of the text.

METHODOLOGY

Moraine Mapping

To constrain the extent of the most recent glaciation, and to establish context for the lake core sediment records, we mapped ice limits for Pinedale and post-Pinedale glaciers adjacent to Independence Lakes and Lake Cleveland. We mapped the moraines both on air photos and on foot, and transferred them to the Cache Peak and Mount Harrison 7.5' USGS topographic quadrangles (Fig. 1). We distinguished Pinedale-equivalent moraines from older deposits based on several criteria: the degree of weathering and relative abundance of surface boulders; qualitative assessment of surface soil development; presence of closed depressions; and preservation of original moraine morphology and slopes. In general, older moraines in the valleys (most likely related to the Bull Lake glaciation; see abstracts by Welty and Mitchell, this volume) are distinctly older based on these criteria; they are significantly more dissected, less hummocky, more rounded, and often larger or much farther down valley. Within Pinedale moraines in both valleys, complex hummocky terrain, abundance of loose, bouldery surface till, and lack of bedrock exposures suggest the glaciers had heavy debris loads. Especially in the Independence Lakes basin, ice-stagnation terrain indicates much of the retreat was by downwasting rather than organized retreat of the glacier. However, each valley also has a set of well-formed recessional moraines that are the main dams for the lakes we cored. Inside of these Pinedale recessional moraines, small, well-preserved moraines occur below the northern cirque walls in both valleys, apparently recording a minor post-Pinedale glacial readvance (Fig. 1). The distinct flow path and moraine character of the moraines indicate that they formed after the Pinedale glaciers had disappeared entirely.

Trimlines mark the cliffs surrounding the basins, generally separating angular rock faces above from rounded glacially abraded faces below. Striations occur on bedrock benches at the western ends of both cirques, and are

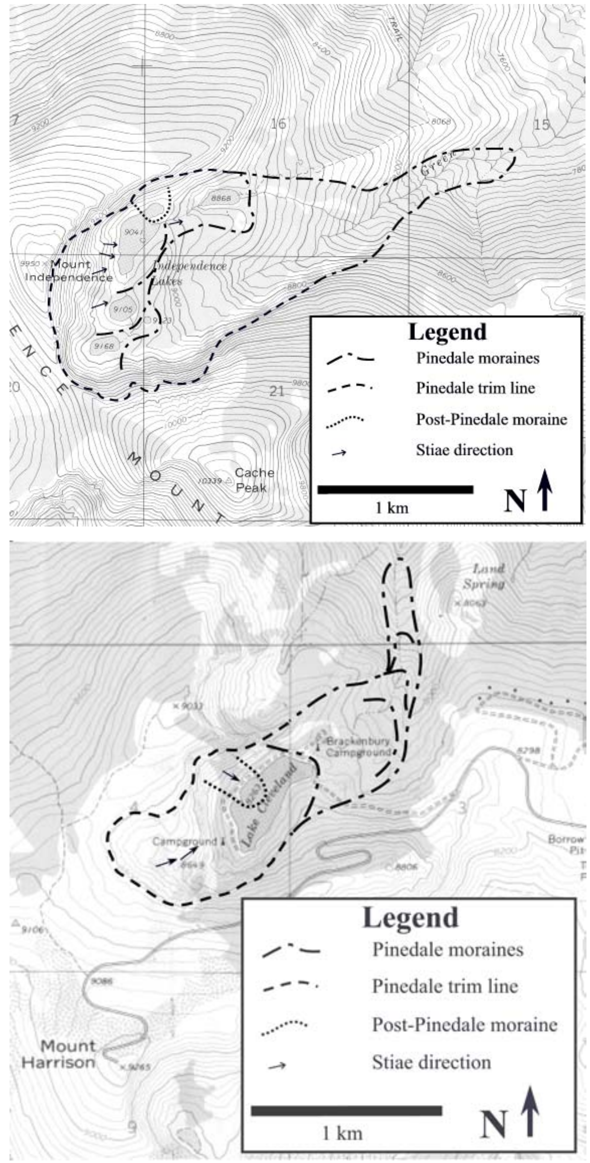

Figure 1. Moraine maps for Independence Lakes and Lake Cleveland cirques. Base maps are Cache Peak and Mount Harrison 7.5' USGS quadrangles.

consistent with expected flow directions based on the geometry of the glacial limits.

Lake Coring

In order to collect the longest, most complete sedimentary records, it is important to core in the deepest part of a lake, or at least in the deepest part of a local basin within a lake. Such basins generally preserve the oldest sediments, and are least likely to have been disrupted by either desiccation or by mass wasting such as slumping or sliding. To ensure we sampled appropriate locations in the lakes, we constructed detailed bathymetric maps of each.

To make the maps, we combined differentially corrected GPS (DGPS) locations using a Timble GeoExplorer 3 and Beacon-on-a-Belt (BoB) differential beacon, with lake-depth measurements using a handheld digital sonar depth finder (PolarVision Strikemaster). Resolution of the DGPS measurements averaged <2 m, whereas the stated resolution of the depth finder is 1.25 inches. Because the depth finder records only in feet, we use those dimensions for depth contours in our bathymetric maps (Fig. 2). To gather the data, teams of two paddled an inflatable canoe in transects across the lake at approximately 6-m intervals. About every 6-m along each transect, the depth was measured and recorded on the GeoExplorers with a DGPS location. This process resulted in a roughly 6x6 m grid of depth control points in each lake. To constrain the lake margins, we walked each shoreline with the GeoExplorer and BoB, recording a location every 5 seconds and assigning each of these points a depth of zero. We transferred the X-Y-Z coordinates of all points into Surfer mapping software (Golden Software, v. 6.04), and created bathymetric maps for each lake (Fig. 2a, b, c).

Maximum lake depths vary from 9 ft (~2.7 m) in Independence Lake 1, to 31 ft (~9.5 m) in Independence Lake 2, to 60 ft. (~18.2 m) in Lake Cleveland. The lattermost constraint has inadvertently dispelled a local legend that Lake Cleveland is “bottomless.” The bathymetry also shows the complexity of the larger two lakes. Whereas Independence Lake 1 has a relatively simple single basin (Fig. 2a)(as do Independence Lakes 3 and 4, not shown here), both Independence Lake 2 and Lake Cleveland have multiple basins. Independence Lake 2 has a large, deep central basin, and a much smaller secondary basin at its eastern end (Fig. 2b). The secondary basin is formed inside the small moraines that comprise the last glacial advance in the basin (Fig. 1). Lake Cleveland is the most complex, with three sub-basins: two deep pockets near the north end, and a shallower basin immediately southeast (and outside) of the small moraines that relate to the latest glacial advance in that basin.

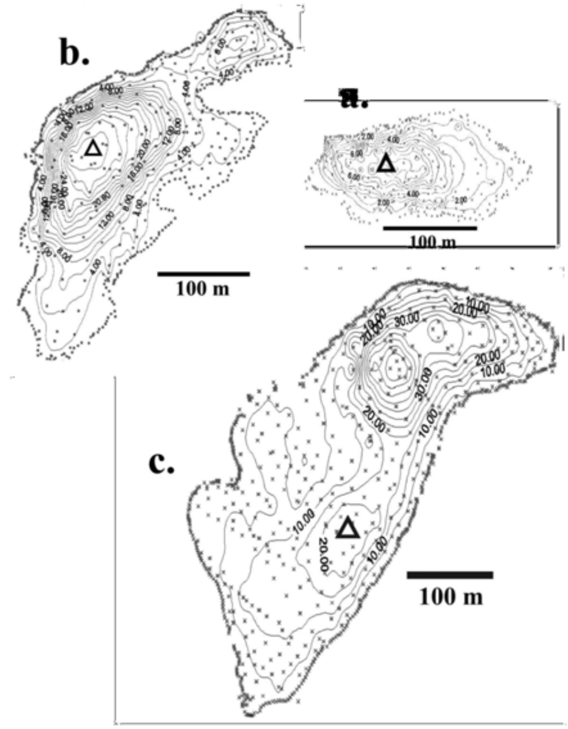

Figure 2. Bathymetric maps of lakes cored in study (see Fig. 1): a. Independence Lake 1; b. Independence Lake 2; c. Lake Cleveland. Bathymetric contour intervals are 1 ft (~0.3 m) for Independence Lake 1 (a), 2 ft (~0.6 m) for Independence Lake 2 (b), and 5 ft. (~1.5 m) for Lake Cleveland (c). Location of depth control points shown by small crosses; locations for cores IL102-1, IL202-1, and LC02-1 indicated by triangles in a, b, and c, respectively. Scale for each lake indicated. North is up for all lakes.

Based on these maps, we cored the deepest basin in each lake except for Lake Cleveland. The two deepest basins in Lake Cleveland proved too deep to core because we could not adequately anchor our coring platform. The Livingston core rods and casing also flexed significantly in the water column, preventing repeated pushes into a single hole. As a result, we cored the shallower sub-basin (23 ft; ~7 m deep) immediately outside (east of) the small moraine loop there (Fig. 1, 2c).

Magnetic susceptibility

We measured magnetic susceptibility (MS) both in the field and in the laboratory with a Bartington MS2C core-scanning susceptibility meter. Readings were taken every 2 cm at a resolution of either 1.0 or 0.1 SI units, depending on the magnitude of values in the core (Fig. 3). The uppermost and lowermost readings collected from each push were eliminated from the graphed data because they are artificially low as a result of edge effects.

Magnetic susceptibility provides a quantitative measure of abundance of magnetic minerals in alpine lake sediments. Depending on local bedrock lithologies, higher MS typically corresponds to greater abundances of clastic sediment, whereas low MS depicts greater organic content; consequently, peaks in magnetic susceptibility are commonly associated with increased glacial or slope-wash activity upstream. Glacial erosion has a particularly strong effect on MS because of its production of unweathered magnetic minerals-bearing glacial flour (e.g., Clark and Gillespie, 1997). Susceptibility variations are greatest near the bottom of all three cores, where fluctuations in clastic vs. organic sedimentation record the latest glacial activity in the Albion Range (Fig. 3). Particularly important are several peaks and troughs at the bottom of cores from both Independence Lake 1 and Lake Cleveland. The MS troughs coincide with more organic layers in both the visual stratigraphy, and in the organic carbon analyses (see section below). These fluctuations appear to represent latest Pleistocene advances that formed the small moraines upstream of both core sites (Fig. 1).

Peaks in MS are also associated with tephra deposits, owing to their inorganic character and magnetic mineral content; the presence of Mazama tephra in each core is indicated by a spike in MS. The remaining Holocene sediments generally have consistently low MS values. However, it is notable that MS values increase near the top of core IL102-1; this change may reflect increased erosion upstream related to regional cooling associated with late-Holocene Neoglaciation and/or the Little Ice Age. Absence of similar trends in the other cores makes this interpretation tentative, though.

Dating control

To establish age control for the sediment cores, we collected macrofossils and bulk organic samples for radiocarbon dating near significant stratigraphic transitions. The samples were dried and processed for AMS-radiocarbon analyses by Team Mud at the Center for Accelerator Mass Spectrometry, Lawrence Livermore National Laboratory. We obtained nine dates for IL102-1, four for IL202-2, and three for LC02-2 (Table 1). Basal samples are from the lowest organic horizons in each core, which provide minimum ages for deglaciation of each lake. All samples are corrected for ^{13}C fractionation and include 1-sigma analytic error ranges. Radiocarbon ages were calibrated with CALIB version 4.3 (Stuiver et al., 1998). The presence of the Mazama tephra, from Crater Lake, in all cores provides an additional age constraint (~6,850 ^{14}C yr B.P.; ~7670 cal yr B.P.). In all cases, radiocarbon dates are in stratigraphic order, internally consistent, and agree with independent age control (e.g., tephras).

1. ELA AND CLIMATE RECONSTRUCTION

(DANIEL CADOL)

This section describes climate reconstructions for the Albion Range, based on the extent of late-Pleistocene glacial deposits. I combine our mapped moraine limits for the Pinedale glaciers below Independence Mountain and Mount Harrison, with known characteristics of modern alpine glaciers to estimate equilibrium-line altitudes (ELAs) and climate conditions at both sites during the last glacial maximum. Our study focused on two different glacial advances in each valley: large Pinedale-maximum glaciers that left behind several lakes and extensive moraines in both valleys, and small post-Pinedale cirque glaciers that originated on steep, south to southeast facing cliffs, and left behind small terminal moraines.

Methods

For this section, I rely on the moraine mapping described above, and topographic controls from the Cache Peak and Mount Harrison USGS 7.5’ quadrangles (Fig. 1). Historical climate data are from the National Water and Climate Center and the Idaho Snow Survey (NRCS NWCC, 2003; NRCS ISS 2003).

E.L.A. Reconstructions

ELA estimates for former glaciers are often based on the *accumulation-area ratio* (AAR) method. In this method the calculations assume that the zone of accumulation is a fixed ratio of the glacier as a whole. This ratio is usually estimated at 0.5-0.8, but can be as low as 0.1 in the case of debris-covered glaciers (e.g., Clark et al., 1994). Most studies assume 2/3 (0.65) of the glacier is in the zone of accumulation. However, more accurate ELA estimates can be obtained by using a spreadsheet developed by Benn and Gemmell (1997). This spreadsheet is based on the *balance-ratio method* of Furbish and Andrews (1984). It takes into account both the hypsometry (how the area of the glacier changes with altitude) and the mass-balance gradient above and below the ELA. To create a hypsometric curve for the Independence Mountain and Mount Harrison glaciers it was first necessary to digitize the moraine maps. I then reconstructed and measured the area of the former glacier surface for every 100ft altitude zone. These data were entered into Benn and Gemmell's spreadsheet.

We use a value of 1.5 for the mass-balance ratio (accumulation gradient/ablation gradient) of all glaciers. This implies that the mass balance gradient in the ablation zone is 1.5 times higher than the mass balance gradient in the accumulation zone, which is the case assuming that the AAR approximates the standard 2/3 value. The assumption that the AAR is about 2/3 for the Pinedale maximum glaciers is supported by the field observation that the transition from trim lines to lateral moraines occurs at about 2570 m (8440 ft) elevation in the Mount Harrison basin, which would make the ablation zone about 1/3 of the area of that glacier.

These parameters resulted in calculated balance-ratio ELAs of 2720 m (8880 ft) for the Independence Mountain Pinedale glacier, and 2540 m (8320 ft) for the Mount Harrison Pinedale glacier. Calculated ELAs for the small post-Pinedale glaciers were 2780 m (9130 ft) and 2550 m (8360 ft), respectively. Like nearly all cirque glaciers (e.g., Clark et al. 1994), the existence of the small post-Pinedale glaciers was likely strongly dependent on enhanced accumulation and decreased ablation related to windblown snow and topographic shading, respectively. Such conditions allowed them to form at lower altitudes and warmer climates than would be possible for a less protected glacier. If this is the case, then the mass-balance ratio was likely higher because of irregular accumulation and a weaker relationship between accumulation and altitude.

Modern Climate Trends

In order to establish modern climate conditions at the elevation of the proposed former ELAs, data were collected from two US Forest Service SNOTEL sites in the Albion Range, and National Weather Service stations in three nearby towns (NRCS NWCC, 2003; NRCS ISS 2003). The two primary climate factors in determining glacial health are average summer (June-August) temperature and average winter moisture accumulation (October-May)(Leonard, 1989). Linear trends to these data when plotted against altitude allow us to estimate modern climate conditions at the elevations of the calculated ELAs (Fig. 4). According to these trends, at the estimated ELA of the Mt. Harrison Pinedale glacier, an average of 74 cm of snow accumulates each winter, and mean summer temperatures average 11.6°C. At the estimated ELA of the Independence Mountain Pinedale glacier, an average of 83 cm of moisture accumulates each winter, and mean summer temperatures average 10.5°C.

Climate Reconstruction

In order to reconstruct the change in climate in the two valleys during the height of the Pinedale glaciation, we compare the modern conditions at the former ELAs to conditions at the ELAs of modern glaciers. Based on modern glaciers, Leonard (1989) proposed an envelope of conditions that support glaciation (Fig. 5). The estimated modern conditions at the Pinedale ELAs plot in the lower right corner of the diagram. In order to move the climate conditions into the glacial zone (i.e., "grow" the glacier), the region must have been cooler in the summer, wetter in the winter, or most likely some combination of both.

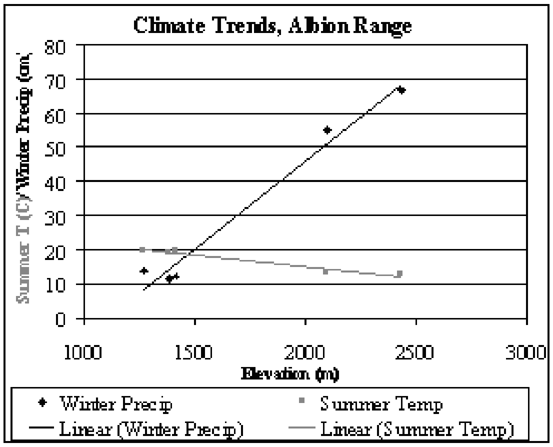

Figure 4. Winter accumulation (October-March) versus summer mean temperatures (June-August) from Leonard (1989). Black dots represent conditions at the equilibrium lines of 32 modern glaciers from around the world. Black lines indicate the range of conditions. Grey dots represent modern conditions at Pinedale ELAs in Albion Range.

If winter precipitation is held constant, summer temperature would have to have been about 7.8°C cooler at Independence Mountain, and 8.4°C cooler at Mt. Harrison. If summer temperature is held constant, winter precipitation would have to have been about 350 cm greater at Independence Mountain, and 500 cm greater at Mt. Harrison. However, by varying both temperature and precipitation, the shortest path to the glacial envelope suggests conditions that were 5.8°C cooler and 60 cm wetter at Independence Mountain, and 6.3°C cooler and 70 cm wetter at Mt. Harrison.

Interpretations

There is a similarity of change required for the two glacial basins when both temperature and precipitation are allowed to vary, more so than when only one factor is taken into account. Also the magnitude of the changes are moderated. Varying both temperature and precipitation appears to give a more coherent picture than temperature or precipitation alone. This finding suggests that the climate was about 6°C cooler and 80-90% wetter than today in the Albion Range at the Pinedale maximum. This suggested change is comparable to other climate reconstructions in the western U.S. (Leonard, 1989; Webb and Bryson, 1972).

2. GRAIN-SIZE ANALYSES OF LAKE SEDIMENTS

(NICOLE BOWERMAN)

Grain-size variations in lake sediments reflect changes in the processes and energy of sediment transport in a watershed. Increased grain sizes generally correspond to higher energy conditions of sediment production or transport, whereas decreased grain sizes indicate decreased activity. Certain processes (e.g. glacial abrasion) also produce characteristic sediments (e.g., rock flour; e.g., Matthews et al., 2000).

To evaluate these changes since the end of the last glaciation in the highest parts of the Albion Range, we analyzed in detail the three longest sediment cores from Lake Cleveland and Independence Lakes. In particular, episodes in which glaciers were present upstream of a lake are indicated by both visual stratigraphy and abundance of silt-sized rock flour produced by glacial abrasion. In post-glacial sediments, grain-size fluctuations, particularly increases in sand sizes, may reflect enhanced slopewash related to increased spring or summer storminess (Noren

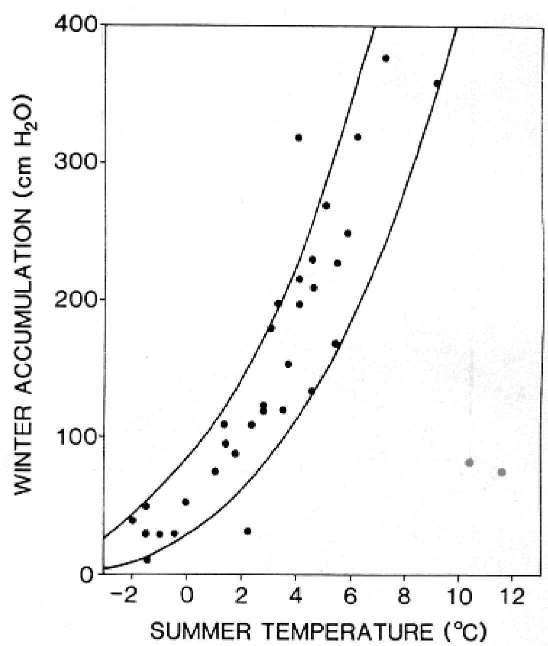

Figure 5. Modern Climate lapse rates in the Albion Range, based on historical averages. Records from the US Department of Agriculture, Natural Resource Conservation Service (NRCS NWCC, 2003; NRCS ISS, 2003).

et al., 2002). Conversely, intervals of decreased grain size indicate either drier summer conditions (less runoff) or at least more consistent weather conditions. The analyses presented here complement our other analyses of the cores, including visual stratigraphy, magnetic susceptibility and organic carbon content.

Methods

Once the cores were split, logged and photographed, samples were collected for organic carbon content, radiocarbon analyses, and particle size analyses. Sampling intervals for carbon content and grain-size analysis through the low-organic silts and transitions to the higher organic muds were spaced approximately every 3 cm in order to assess the changes indicated by the visual stratigraphy. Because the stratigraphy was less variable higher in the cores, samples were only taken every 15 cm throughout the upper organic muds (gyttja). One cc of sediment was taken for each grain size sample and pretreated with hydrogen peroxide to remove organic sediments. After this pretreatment, several samples from core IL202-2 still contained a white, amorphous, low-density substance that floated above of the settled sediment. Examination under a Scanning Electron Microscope (SEM) indicated that the material was mainly decomposed wood fragments and diatoms. To remove these non-clastic components, all samples were then pretreated with NaOH. When all pretreatment was complete, the samples were analyzed for particle size characterization using a Malvern Mastersizer 2000 laser particle size analyzer with Autosampler. This system measures volumetric grain sizes from 0.01-2000 microns with a high degree of accuracy.

Results

In all cores, silts are the dominant clastic grain size, comprising >50% of the sediments throughout (Fig. 3). Clays typically comprise 15-20% of the cores, increasing slightly in the Holocene sediments, whereas sands show the greatest variability, ranging from negligible amounts to ~25%.

Grain sizes in core IL102-1, from the lowest of the four Independence Lakes, display the largest and most rapid fluctuations in grain size of the three cores (Fig. 3a). Variations in grain size appear to be controlled primarily by the very-fine to fine sand component. A spike of medium-to-coarse silt at the base of the core decreases rapidly upward as sand and fine silts expand. Between this basal layer and the Mazama tephra (275 cm), the core is characterized by fluctuations of sand content between 0 and 20%. Above the tephra, the sand content generally remains between 8-15% with two notable exceptions at 245 cm (~5600 ^{14}C yr B.P.; ~6400 cal yr B.P.) and 165 cm (~3900 ^{14}C yr B.P.; ~4400 cal yr B.P.), where it disappears completely. Silt-sized particles remain reasonably consistent relative to the sand whereas there is a gradual ~5% increase in clay particles upward in the core.

Core IL202-2, collected from the second and largest of the four Independence Lakes, provides the shortest record of the three cores (Fig. 3b). The grain size variations in this core also appear to be dictated mainly by changes in the sand content. However, the core displays relatively few and subtle grain-size fluctuations, in part because the core is entirely Holocene in age, and consists mainly of organic-rich sediments. Broad millennial-scale changes in sand content range between 10% to 20%, with the lowermost 15 cm of the core bottoming in a decrease in grain size. As indicated by the basal date (9715 ± 50 ^{14}C yr BP; ~11,150 cal yr B.P.), the core does not record the older, more variable late-Pleistocene outwash sediments present in the other cores.

Grain sizes in core LC02-2, from the northeastern half of Lake Cleveland, display a subtle but significant general fining-upward trend, with more rapid fluctuations (partly reflecting denser sampling) in the bottom third of the core where low-organic silts dominate (Fig. 3c). Similar to core IL102-1, grain-size variations in the low-organic sediments below ~275 cm (11,630 ± 45 ^{14}C yr B.P.; ~13,640 cal yr B.P.) appear to be dictated mainly by fluctuations in the sand-sized particles, although medium and coarse silts also co-vary with the sand.

Interpretations

Abundance in silt-sized particles, particularly blue-gray silts (rock flour), indicates activity of upstream glaciers. Fluctuations in silt-sized particles within the low-organic intervals therefore appear to record variations in glacier extent upstream. Low-organic silts in the lower parts of cores IL102-1 (Independence Lake 1) and LC02-2 (Lake Cleveland) record both the retreat of the Pinedale glaciers past the lakes, as well as the last-gasp readvance indicated by the small moraines upvalley of both coring sites (Fig. 1).

In both cores, the basal decrease in silt records the demise of the Pinedale glaciers (sometime before 13,020 ± 50 ^{14}C yr B.P.; ~15,400 cal yr B.P.). Fluctuations in silt above the base appear to record minor glacial activity above the core sites, probably related to formation of the small upvalley moraines. Increases in silt near the transition to organic mud in both cores, coincident with less-organic layers and small spikes in MS (Fig. 3a, c), may record the last glacial activity in each valley. The transition to organic-rich mud and general increases in grain size at 423 cm in IL102-1 and at 280 cm in LC02-1 record the final demise of glaciers in the Albion Range. The date of this transition is essentially the same in both cores: ~11,800 ^{14}C yr B.P. (~13,800 cal yr B.P.; interpolated) for IL102-1, and 11,630 ± 45 ^{14}C yr B.P. (~13,640 cal yr B.P.) for LC02-1. IL202-2 does not preserve substantial thicknesses of glacial silt, but the age of the organic sediment immediately above the thin basal layer of blue-gray silt is generally consistent with the dates above the glacial silt in the other two cores.

The Holocene (non-glacial) sediments do not display any large peaks in coarse grain size that might be associated with dramatic shifts in runoff conditions; however, all cores show broad intervals of increased grain sizes in the early Holocene (pre-Mazama), between Mazama and ~3800 ^{14}C yr B.P., and near the top of each core (Fig. 3). These intervals may correspond to periods of increased wet weather conditions during the spring and summer seasons.

3. ORGANIC CARBON ANALYSES OF LAKE SEDIMENTS

(PAUL BOVET)

The organic carbon content of sediment cores from lakes in the Albion Range provides a potentially rich record of late Pleistocene and Holocene environmental change. The lake sediment in a glaciated valley can be seen as a record of climatically-influenced geomorphic activity upvalley. During cold and/or moist intervals, periglacial and possibly glacial processes are enhanced and accelerated, which is likely to increase clastic sediment supply to the lake. At the same time, cold conditions should lead to a decrease in organic productivity within the lake and in the surrounding drainage. As a result, colder periods would be expected to produce lake sediments with low concentrations of organic carbon. Based on these scenarios, we are able to follow subtle alterations of paleoenvironmental conditions through the analysis of organic carbon content.

Methods

We analyzed organic carbon content in the three longest cores discussed previously: LC02-2, IL102-1, and IL202-2 (Fig. 2, 3). Samples were collected at the same intervals as for the particle size analysis. Total carbon content of the samples was determined by pyrolysis using a UIC CM 5012 CO_2 callometer. The total carbon content measurements are assumed to be a close approximation of the organic carbon content, because the sediment contains little or no inorganic carbon. There is no carbonate bedrock in the Independence Lakes drainage. A small area of carbonate bedrock is present east of Lake Cleveland, but acid digestion analysis of samples from core LC02-2 indicated no detectable amounts of inorganic carbon.

Results

This section focuses on our results in core IL102-1 from Independence Lake #1 because its record of environmental change is longest and best constrained by ^{14}C dates. The stratigraphy of the core is discussed earlier.

The basal gray silt in core IL102-1, from 478–424 cm, contains less than 1% organic carbon throughout the section (Fig. 3a). Based on interpolation between several radiocarbon dates (Table 1), this interval was deposited between ~11,800 ^{14}C yr B.P. (~13,800 cal yr B.P.; interpolated) to >13,020 ± 50 ^{14}C yr B.P. (~15,400 cal yr B.P.). Immediately overlying this section, organic carbon increases sharply, peaking around 15% at a core depth of 370 cm. This peak is relatively well constrained between AMS ages of 9925 ± 40 ^{14}C yr. B.P. (~11,280 cal yr B.P.) and 8330 ± 60 ^{14}C yr. B.P. (~9300 cal yr B.P.). Organic carbon content progressively declines upward for about 80–90 cm above the peak, until it reaches organic carbon levels around 7-8%. Mazama tephra (~6850 ^{14}C yr B.P.) is present in the core at 280 cm – 260 cm. Organic carbon content of core sediments post-dating Mazama tephra remains relatively constant, varying from 6% - 11%, averaging ~8%. There are no clear trends in organic carbon content in this upper section of the core. However, two outliers within this section drop significantly below the average. A single measurement at 140 cm, just above an AMS age of 3875 ± 40 ^{14}C yr. B.P. (~4310 cal yr B.P.), contained 5% organic carbon. This sample, contains glass shards of what is probably St. Helens Y tephra (3,300-3400 ^{14}C yr B.P.)(Mullineaux, 1996). The other outlier comes from a single measurement at 45 cm containing 4.5% organic carbon. This sample contained no glass shards, thus its low organic content cannot be attributed to tephra influx.

Organic carbon profiles of core IL202-2 and core LC02-2 closely resemble that of core IL102-1, although the chronologies of these two cores are less well constrained. As with core IL102-1, these two cores bottom in relatively inorganic basal gray silt. Above this layer organic carbon increases sharply to a pre-Mazama peak, falling again to intermediate levels shortly before deposition of the Mazama Ash. Intermediate levels persist to the top of all three cores. However, there are a few differences between cores. Ages of the high peak in organic carbon differ by ~400 years between core IL102-1 at 8330 ± 60 ^{14}C yr. B.P. (~9300 cal yr B.P.) and LC02-2 at 8750 ± 40 ^{14}C yr. B.P. (~9750 cal yr B.P.). The rate of sediment accumulation differs between all three cores, causing similar events, i.e. Mazama tephra, to appear at different depths (Fig. 3a-c). There are also differences in the average organic carbon content between lakes most likely due to the filtering of inorganic clastic sediment by upvalley lakes in the Independence Lake system. Lake Cleveland is the only lake in its basin, allowing clastic sediment to accumulate into it more directly.

Interpretations

Based on an AMS date near the bottom of core IL102-1, deglaciation of the Independence Lakes occurred by 13020 ± 50 ^{14}C yr. B.P. (~15,400 cal yr B.P.). The gray inorganic silt at their bases is therefore either the result of direct upvalley glacial outwash or periglacial sediment (Church & Ryder, 1972). In the former case, the abrupt change from gray silt to gyttja in all three lakes may mark the final recession of ice within the cirques of Independence lakes and Lake Cleveland. However, if the gray silt is periglacial, the change would postdate the final recession of ice but indicate an abrupt warming leading to increased biological productivity within the lakes and vegetative stabilization of periglacial and glacial deposits in the tributary basins. The peak in organic carbon above this horizon indicates a substantial increase in plant growth within and around the lakes. This peak is interpreted as being the result of the Altithermal warm interval in the early to mid-Holocene. In the upper half of the three cores, organic carbon levels remain relatively constant, indicating a generally stable climate of moderately warm temperatures, close to present day levels, and little periglacial geomorphic activity upvalley. Core LC02-2 is the only core of the three that records a significant shift in the upper sediments. Organic carbon levels in LC02-2 above Mazama ash but below sediments dated 2550 ± 45 ^{14}C yr. BP (~2610 cal yr B.P.) decrease upward to an average just above 3% from a previous average around 4% above. This may indicate a minor climatic change toward more periglacial conditions coincident with Neoglaciation elsewhere in the western U.S.

CONCLUSIONS

Our study provides the first detailed assessment of post-glacial environmental change in the Albion Range. Reconstructions of glacial snowlines suggest that at the height of the Pinedale glaciation, summer temperatures in the cirques were approximately 6 degrees cooler, and winter precipitation was ~80-90% greater, than at present. Radiocarbon dates from sediment cores of lakes near the cirques demonstrate that Pinedale deglaciation was nearly complete by 13,020 ± 50 ^{14}C yr B.P. (~15,400 cal. yr B.P.). A coeval increase in both magnetic susceptibility and clastic sand, and a decrease in organic carbon content, in the cores indicate that final deglaciation of the Albion Range occurred by ~11,630 ± 45 ^{14}C yr B.P. (~13,640 cal yr B.P.). The sediment analyses also indicate that the readvance of small post-Pleistocene glaciers in each cirque occurred between ~13,020 ± 50 ^{14}C yr B.P. (~15,400 cal. yr B.P.) and ~11,630 ± 45 ^{14}C yr B.P. (~13,640 cal yr B.P.). This sequence of deglaciation and readvance is similar to events recorded in the Sierra Nevada (Clark and Gillespie, 1997). It also implies the absence of glaciation during the Younger Dryas, a cold event that is recorded by glacier readvances in the Rocky Mountains (e.g. Menounos and Reasoner, 1997).

REFERENCES CITED

Benn, Douglas I. and Gemmell, Alastair M.D. 1997, Calculating equilibrium-line altitudes of former glaciers by the balance ration method: a new computer spreadsheet. Glacial Geology and Geomorphology. http://ggg .qub.ac.uk/ ggg/papers/full/1997/tn011997/tn01.html

Church, M., and Ryder, J.M. (1972). Paraglacial sedimentation: A consideration of fluvial processes conditioned by glaciation. Geological Society of America Bulletin, 83, 3059-3071.

Clark, D.H., Clark, M.M. and Gillespie, A.R. 1994. Debris-covered glaciers in the Sierra Nevada, California, and their implications for snowline reconstructions. Quaternary Research, 41: 139-153.

Clark, D.H. and Gillespie, A.R., 1997: Timing and significance of late-glaciation and Holocene cirque glaciation in the Sierra Nevada, California. Quaternary International, vol. 38/39, pp. 21-38.

Leonard, Eric M., 1989, Climatic change in the Colorado Rocky Mountains: Estimates based on modern climate at Late Pleistocene equilibrium lines. Arctic and Alpine Research, vol. 21, no 3, pp. 245-255.

Matthews, John A., Svein Olaf Dahl, Atle Nesje, Mark S. Berrisford, and Carin Andersson, 2000, Holocene glacier variations in central Jotunheimen, southern Norway based on distal glaciolacustrine sediment cores. Quaternary Science Reviews, vol. 19, pp. 1625-1647

Menounos, B. and Reasoner, M.A., 1997: Evidence for cirque glaciation in the Colorado Front Range during the Younger Dryas chronozone. Quaternary Research, vol. 48, pp. 38-47.

Mullineaux, D. (1996). Pre-1980 tephra-fall deposits erupted from Mount St. Helens, Washington. USGS Professional Paper, #1563.

Noren, Anders J., Paul R. Bierman, Eric J. Steig, Andrea Lini and John Southon, 2002, Millenial-scale storminess variability in the northeastern United Stated during the Holocene epoch. Nature, vol. 419, pp. 821-824

NRCS ISS. Howell Canyon and Magic Mountain SNO-TEL site data. http://www.id.nrcs.usda.gov/ snow/snotel/hist-id-snotel.htm

NRCS NWCC. Burley, Malta, and Oakley taps data. http://www.wcc.nrcs.usda.gov/water/climate/climchoice.pl?state=id&county=16031

Stuiver et al., (1998), CALIB Radiocarbon Calibration. http://depts.Washington.edu/qil/calib/, version 4.2

Webb, T. and Bryson, R.A. 1972. Late- and Postglacial Climate Change in the Northern Midwest, USA: Quantitative Estimates Derived from Fossil Pollen Spectra by Multivariate Statistical Analysis. Quaternary Research, vol. 2, pp. 70-115.

ACKNOWLEDGEMENTS

Team Mud would like to acknowledge all the 2002 Idaho project participants for their help in backpacking the raft and coring equipment up to the Independence Lakes, and perhaps more importantly, back out of the lakes! We could not have done it without you.

Table 1. Radiocarbon Dates, cores IL102 -1, IL202-2, and LC02-2

CAMS #	Sample Name	Depth (cm)	Sample type	Stratig. Significance	^{14}C age	±	2-sigma Cal age BP (Probability)*	Best-guess Cal Age
92762	IL102-1-2 C1A	156	macrofossil	transition to lighter seds above	3875	35	4412 - 4228 (0.914) 4201 - 4180 (0.051) 4171 - 4157 (0.035)	4310
92763	IL102-1-3 C4	235	pineneedle	~38cm above Mazama	5510	40	6401 - 6360 (0.214) 6356 - 6271 (0.631) 6239 - 6203 (0.155)	6320
92764	IL102-1-4 C7	359.5	twig	next to light stripe (diatoms?)	8330	60	9486 - 9237 (0.885) 9219 - 9185 (0.034) 9178 - 9132 (0.081)	9300
92765	IL102-1-5 C9	404	twig	~18 cm above outwash	9925	40	11549 - 11503 (0.140) 11480 - 11474 (0.010) 11421 - 11386 (0.057) 11355 - 11203 (0.794)	11,280
92833	IL102-1-5 C9rep	404	twig	~18 cm above outwash	9885	35	11332 - 11322 (0.051) 11300 - 11199 (0.949)	11,250
93767	IL102-1-5 C10	404	bulk sed	~18 cm above outwash	9585	35	11119 - 10739 (1.000)	10,930
92766	IL102-1-5 C11	433.5	bulk sed	inter-outwash	12820	60	15819 - 14418 (1.000)	15,120
92834	IL102-1-5 C11rep	433.5	bulk sed	inter-outwash	12810	40	15799 - 14419 (1.000)	15,110
92767	IL102-1-6 C12	452.5	bulk sed	inter-outwash	13020	50	16110 - 14675 (1.000)	15,400
92768	IL202-2-3 C7	186.5	seed	gyttja	3730	40	4227 - 4202 (0.048) 4178 - 4171(0.013) 4159 - 3973 (0.923) 3941 - 3932 (0.016)	4070
92769	IL202-2-4 C11	303	wood	gyttja above Mazama	6260	45	7267 - 7147 (0.647) 7129 - 7019 (0.353)	7210
92770	IL202-2-6 C14	461	bulk orgs	light layer between light layers	9530	35	11086 - 10934 (0.503) 10893 - 10886 (0.007) 10876 - 10685 (0.490)	11,010 or 10,870
92802	IL202-2-6 C15	474	bulk sed	lowest orgs above basal rock	9715	50	11226 - 11064 (0.793) 10942 - 10856 (0.181) 10824 - 10794 (0.026)	11,150
92771	LC02-2-2 C11	101	twig	gyttja	2550	45	2758 - 2469 (1.000)	2610
92772	LC02-2-4 C1	236	wood	above org-rich layer	8750	40	9908 - 9594 (0.973) 9579 - 9566 (0.027)	9750
92803	LC02-2-4 C5	279	macrofossil	between light-gray layers	11630	45	13859 - 13415 (1.000)	13,640

* Stuiver et al., 1998

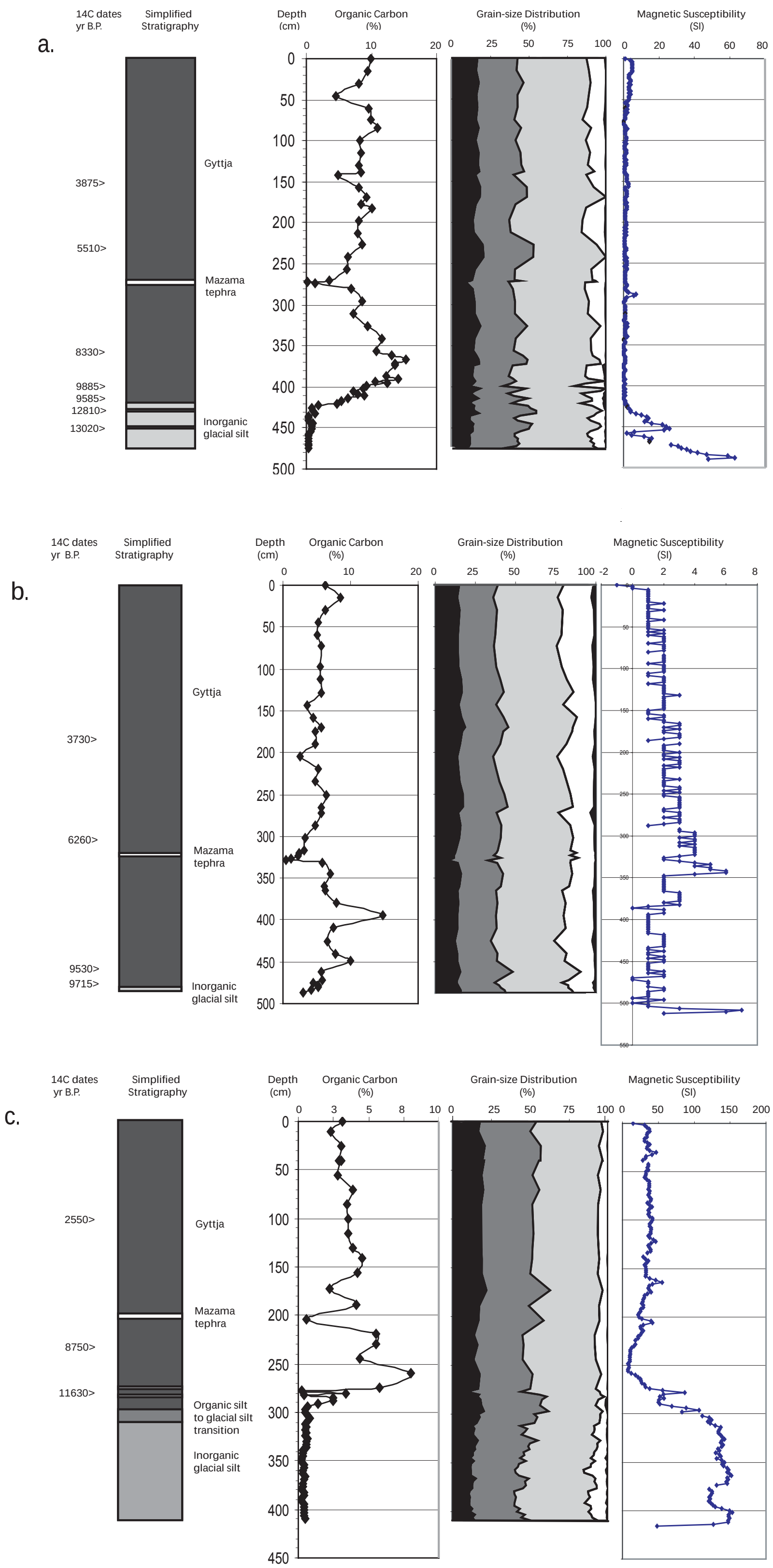

Figure 3. Core stratigraphy of a) IL102-2, b) IL202-2, and c) LC02-2: radiocarbon dates, simplified stratigraphy, organic carbon content, grain size distribution (ordered left to right: clay, very fine-fine silt, med-coarse silt, very fine-fine sand and med sand) and magnetic susceptibility.